

See discussions, stats, and author profiles for this publication at: <http://www.researchgate.net/publication/264745748>

Optimizing Regions-of-Interest Composites for Capturing Treatment Effects on Brain Amyloid in Clinical Trials.

ARTICLE *in* JOURNAL OF ALZHEIMER'S DISEASE: JAD · AUGUST 2014

Impact Factor: 4.15 · DOI: 10.3233/JAD-131979 · Source: PubMed

CITATION

1

READS

20

6 AUTHORS, INCLUDING:



Volha Tryputsen

Janssen Research & Development, LLC

4 PUBLICATIONS 2 CITATIONS

SEE PROFILE



Allitia Dibernardo

Novartis

22 PUBLICATIONS 312 CITATIONS

SEE PROFILE



Nandini Raghavan

Johnson & Johnson

45 PUBLICATIONS 282 CITATIONS

SEE PROFILE

Optimizing Regions-of-Interest Composites for Capturing Treatment Effects on Brain Amyloid in Clinical Trials

Volha Tryputsen*, Allitia DiBernardo, Mahesh Samtani, Gerald P. Novak, Vaibhav A. Narayan, Nandini Raghavan and the Alzheimer's Disease Neuroimaging Initiative¹
Janssen Research & Development LLC, Pharmaceutical Companies of Johnson & Johnson, USA

Handling Associate Editor: Tim Schultz

Accepted 28 June 2014

Abstract.

Background: Pittsburgh Compound B (PiB) positron emission tomography (PET) neuroimaging is a powerful research tool to characterize amyloid evolution in the brain. Quantification of amyloid load critically depends on (i) the choice of a reference region (RR) and (ii) on the selection of regions of interest (ROIs) to derive the standard uptake value ratios (SUVRs).

Objective: To evaluate the stability, i.e., negligible amyloid accumulation over time, of different RRs, and the performance of different PiB summary measures defined by selected ROIs and RRs for their sensitivity to detecting longitudinal change in amyloid burden.

Methods: To evaluate RRs, cross-sectional and longitudinal analyses of focal regional and composite measures of amyloid accumulation were carried out on the standardized PiB-PET regional data for cerebellar grey matter (CER), subcortical white matter (SWM), and pons (PON). RRs and candidate composite SUVR measures were further evaluated to select regions and develop novel composites, using standardized 2-year change from baseline.

Results: Longitudinal trajectories of PiB4—average of anterior cingulate (ACG), frontal cortex (FRC), parietal cortex, and precuneus—demonstrated marked variability and small change from baseline when normalized to CER, larger changes and less variability when normalized to SWM, which was further enhanced for the composite in PON-normalized settings. Novel composite PiB3, comprised of the average SUVRS of lateral temporal cortex, ACG, and FRC was created.

Conclusion: PON and SWM appeared to be more stable RRs than the CER. PiB3 showed compelling sample size reduction and gains in power calculations for clinical trials over conventional PiB4 composite.

Keywords: Alzheimer's disease, amyloid imaging, brain, pons, ¹¹C-PiB

INTRODUCTION

Positron emission tomography (PET) neuroimaging with amyloid ligands has allowed *in vivo* visualization of amyloid plaques, a core molecular feature of Alzheimer's disease (AD) pathology. The first amyloid tracer used in humans, ¹¹C-6-OH-BTA, conventionally known as Pittsburgh Compound B tracer (PiB) [1], shows high specificity for insoluble amyloid fibrils [2] in postmortem brain tissue and has become a powerful research tool to characterize amyloid evolution in normal aging and people affected with AD or its prodromal states.

*Correspondence to: Volha Tryputsen, Janssen Research & Development, LLC, 1000 US Highway 202, Raritan, NJ 08869, USA. Tel.: +1 908 927 5320; Fax: +1 908 927 3782; E-mail: vtryputsen@its.jnj.com.

¹Data used in preparation of this article were obtained from the Alzheimer's Disease Neuroimaging Initiative (ADNI) database (<http://adni.loni.usc.edu/>). As such, the investigators within the ADNI contributed to the design and implementation of ADNI and/or provided data but did not participate in analysis or writing of this report. A complete listing of ADNI investigators can be found at: http://adni.loni.usc.edu/wp-content/uploads/how_to_apply/ADNI_Acknowledgement_List.pdf

Traditionally, the amount of amyloid plaque present is estimated by quantifying tracer signal intensity in specific regions of interest (ROIs) [3]. Specifically, these usually include the frontal, parietal, and temporal lobes, portions of occipital cortex, and striatum as well as lateral temporal and medial temporal lobes. These regions tend to show significant differences in amyloid binding between AD and healthy controls. Signal intensity within individual ROIs can vary due to the timing of the scan, the tracer load, and other factors. Therefore ROI measurements are standardized to a cerebellar (CER) reference region where amyloid accumulation is thought to be minimal [4]. Longitudinal change over time is assessed as the difference between the ROI/CER ratios over time. Thus the accuracy of longitudinal estimates of amyloid accumulation based on PiB critically depends as much on the assumption of stability of the reference region as on the selection of ROIs to reflect amyloid accumulation (or decrease in the case of anti-amyloid therapies).

There are several important sources of pre-analytical and analytical variability that can challenge the accuracy of longitudinal amyloid measurements with PiB. In this work, we focus on evaluating the stability of several reference regions to identify the one which is optimal for measuring longitudinal change in ROIs. In particular, we hypothesized that the pons (PON) might be more stable than CER, and undertook to study this structure as an alternative reference region. We also evaluated the subcortical white matter (SWM). We further studied the accumulation in various ROIs to develop novel ROI composites with improved sensitivity to capturing change in amyloid burden over time.

METHODS

Data

Data used in the preparation of this article were obtained from the Alzheimer's Disease Neuroimaging Initiative (ADNI) database (<http://adni.loni.usc.edu/>). The ADNI was launched in 2003 by the National Institute on Aging (NIA), the National Institute of Biomedical Imaging and Bioengineering (NIBIB), the Food and Drug Administration (FDA), private pharmaceutical companies and non-profit organizations, as a \$60 million, 5-year public-private partnership. The primary goal of ADNI has been to test whether serial magnetic resonance imaging (MRI), positron emission tomography (PET), other biological markers, and clinical and neuropsychological assessment can be

combined to measure the progression of mild cognitive impairment (MCI) and early Alzheimer's disease (AD). Determination of sensitive and specific markers of very early AD progression is intended to aid researchers and clinicians to develop new treatments and monitor their effectiveness, as well as lessen the time and cost of clinical trials.

The Principal Investigator of this initiative is Michael W. Weiner, MD, VA Medical Center and University of California – San Francisco. ADNI is the result of efforts of many co-investigators from a broad range of academic institutions and private corporations, and subjects have been recruited from over 50 sites across the U.S. and Canada. The initial goal of ADNI was to recruit 800 subjects but ADNI has been followed by ADNI-GO and ADNI-2. To date these three protocols have recruited over 1,500 adults, ages 55 to 90, to participate in the research, consisting of cognitively normal older individuals, people with early or late MCI, and people with early AD. The follow up duration of each group is specified in the protocols for ADNI-1, ADNI-2 and ADNI-GO. Subjects originally recruited for ADNI-1 and ADNI-GO had the option to be followed in ADNI-2. For up-to-date information, see <http://www.adni-info.org/>.

We analyzed 224 [¹¹C] PiB-PET scans of cognitively normal (NL), MCI, and AD clinically diagnosed subjects from the ADNI database. The data was downloaded from the laboratory of neuroimaging (LONI) web-site (<http://adni.loni.usc.edu/>), in July 2011. It included 103 subjects at baseline; 19 meeting clinical criteria for AD, 65 judged to be MCI, and 19 classified as NL at the time of the first cognitive assessment. Of those 103 subjects at baseline, 80 underwent their first PiB-PET assessment at the one year visit and 39 at the two year visit. In particular, since not all subjects had PiB-PET measurements taken at the Baseline visit, in our analysis, we synchronized their clinical diagnosis to the time of first PiB-PET scan. Since six subjects initially classified as MCI progressed to dementia and three reverted to NC by the time they had their first PiB-PET scan, the clinical classification of the 103 subjects at the time of their modified baseline is as follows: 25 AD, 56 MCI, and 22 NL. This latter diagnosis is used to classify subjects in the analysis described in this article.

PiB-PET scans were administered at different sites. Information on acquisition (<http://adni.loni.usc.edu/methods/pet-analysis/pet-acquisition/>), pre-processing (<http://adni.loni.usc.edu/methods/pet-analysis/pre-processing/>), and post-processing procedures (<http://adni.loni.usc.edu/methods/pet-analysis/>) is

available through the LONI website. In our analysis, we used PiB-PET image data analyzed by University of Pittsburgh (U Pitt). The U Pitt data was normalized to gray matter cerebellum prior to taking the mean across each multi-plane ROI. Specifically the ROIs considered here are: 9 cortical ROIs - anterior cingulate (ACG), frontal cortex (FRC), lateral temporal cortex (LTC), parietal cortex (PAR), precuneus cortex (PRC), mesial temporal cortex (MTC), occipital cortex (OCC), occipital pole (OCP), and sensory motor cortex (SMC); 3 sub-cortical ROIs - anterior ventral striatum (AVS), sub-cortical white matter (SWM), thalamus (THL) as well as cerebellum (CER) and pons (PON). Several composites were calculated as a mean PiB uptake across specific ROIs, including a 4-region composite - PiB4 (defined by the anterior cingulate, frontal cortex, parietal cortex, and precuneus). This is the SUVR composite recommended by the ADNI PET Core for measuring amyloid accumulation [5].

Statistical analyses

Comparison of reference regions

We primarily evaluated CER and PON to assess optimal region to serve as a reference. As a secondary analysis, we also evaluated SWM as a potential reference region.

Because ADNI data was already pre-normalized to CER, we converted CER-normalized SUVRs to obtain PON-normalized SUVRs by dividing existing regional SUVR values by SUVR for Pons. This operation made values of PON equal to one and re-normalized all other regional SUVRs to PON. CER-normalized SUVRs were converted to SWM-normalized SUVRs, using the same procedure.

For a cross-sectional evaluation, boxplots were constructed for 13 regional PiB-PET SUVR measures for 8 cross-sectional cohorts (AD at baseline and year 1; MCI and NL at baseline, year 1, and year 2; and the counts of subjects observed at each time point are reported in Table 1) for the three candidate reference regions, CER, PON, and SWM. SUVR distributions were further checked for differences.

We constructed profile plots to examine longitudinal trajectories of amyloid accumulation within each

clinical cohort. This was done for the SUVR of each ROI and for the SUVR composite PiB4.

Summary statistics for the SUVR composite were calculated for each cross-sectional cohort, based on all the subjects available at each time point. Mean longitudinal trajectories of SUVRs and SUVR change from baseline across disease cohorts were found to be informative for further reference region evaluation.

Development of composite ROIs for tracking amyloid deposition

Cutoff thresholds for amyloid positivity for new reference regions: In our analyses, we classified amyloid pathology positive (PiB+) and negative (PiB-) subjects based on a widely-used SUVR cut-off of 1.5 for baseline measurements of CER-normalized PiB4 composite values [6], defining a subject as PiB+ if baseline PiB4, normalized to CER was greater or equal then 1.5 and PiB- if otherwise. To obtain corresponding biomarker cutoffs for the other reference regions considered (PON, SWM) the baseline PiB4 normalized to PON was regressed on the baseline PiB4 normalized to CER, and separately the baseline PiB4 normalized to SWM was regressed on the baseline PiB4 normalized to CER.

Only subjects who met criteria for PiB+ as defined above were included in later analysis, described below. We applied reference-region-specific SUVR cut-offs to CER, PON, and SWM-normalized data separately to subset biomarker positive individuals.

Selection of ROIs for novel composite: A novel summary measure was developed by identifying the ROIs most sensitive to longitudinal change from baseline, using an approach similar to that of Raghavan et al. [12] for developing cognitive composites. The mean 2-year change from baseline was estimated by subtracting baseline SUVR from SUVR at Year 2 visit for each PiB-positive subject for whom 2-year data was available. The standardized mean SUVR 2-year changes from baseline were obtained by dividing the mean 2-year change from baseline by the corresponding standard deviation of 2-year change from baseline [12]. The above estimates of standardized mean change were based on a sample of 21 (for CER and SWM-normalized data) or 20 (for PON-normalized data) PiB-positive subjects.

Plots of standardized 2-year change from Baseline in amyloid from baseline were constructed for each of the individual ROIs and for the PiB4 SUVR composite. This allowed us to: i) Identify regions/composites

Table 1

Number of subjects in each cohort observed at each time point

	Baseline	Year 1	Year 2
Cognitively normal	22	20	12
Mild cognitive impairment	56	44	25
Alzheimer's disease	25	16	2
Total	103	80	39

sensitive to change and with low variability; and ii) Compare among CER, PON, and SWM-normalized SUVR data.

A novel PiB-PET SUVR composite was then created by evaluating the 13 regions listed above across the whole spectrum of disease severity and selecting optimal regions to be included in the composite.

We then compared the utility of this composite versus PiB4 for clinical trial settings by calculating the power to detect a hypothesized 25% treatment effect over 2 years. This was plotted as a function of a sample size comparing between composite measures across 3 normalization methods. The power calculations were based on annual measurements available during the 2-year period and were done through a linear mixed effect model with random slopes for PiB4 and the proposed novel composite.

RESULTS

Comparison of reference regions

Table 2 showed some baseline characteristics of the three subject populations: NL, MCI, and AD. There was no significant difference in age and proportion of women between three groups. AD appeared the most severe in terms of all cognitive measures listed in Table 2.

Figure 1a–c showed boxplots of ROIs referenced to CER, PON, and SWM, respectively. The boxplots in Fig. 1a indicated that the majority of ROIs normalized to CER yielded a pattern where amyloid apparently increased within the region with the increasing severity of the disease (NL<MCI<AD). This pattern was seen for all regions and was consistent with the expectation that amyloid burden increased with increasing severity. However, for the two regions, PON and SWM, both of which should be relatively unaffected by amyloid deposition, a counter-intuitive patterns was noted. In those two regions, when referenced to CER, amy-

loid burden *decreased* with increasing disease severity (AD<MCI<NL).

Similarly, the boxplots in Fig. 1b showed the corresponding boxplots for ROIs normalized to PON. Unlike the counter-intuitive pattern noted above for PON and SWM normalized to CER, we noted here that CER normalized to PON followed the expected pattern, i.e., amyloid deposition *increased* with increasing disease severity (NL<MCI<AD). Further, SWM normalized to PON stayed relatively constant across time and clinical subgroups, in contrast to its behavior when normalized to CER.

In the same fashion, the boxplots in Fig. 1c revealed that amyloid burden in CER *increased* with increasing disease severity when normalized to SWM (NL<MCI<AD). However, PON normalized to SWM stayed relatively constant across time and disease severity unlike its behavior when normalized to CER.

One explanation for these findings is that the CER may have more of amyloid uptake than previously thought. The behaviors of SWM and PON normalized to CER could diverge from other ROIs if these two regions have little or no amyloid and if the CER is in fact accumulating amyloid over time. Note that this was borne out by the corresponding increase in CER amyloid burden with increasing disease severity when normalized to PON, assuming that the PON amyloid burden is stable across the evolution of the disease.

The plots of longitudinal trajectories of PiB4 in Fig. 2 demonstrated marked variability at an individual level for CER, PON, or SWM reference region. Although there was some overlap between the clinical cohorts, the overall pattern of baseline distributions confirmed the expectations with NL having the lowest and AD the highest baseline PiB4. The broadest distribution of baseline values was seen in the MCI group regardless of reference region used.

The plots in Fig. 3a–c showed the mean and 95% confidence interval of PiB4 at each time-point for each clinical cohort (NL (green), MCI (yellow), AD (red))

Table 2
Baseline characteristics of NL, MCI, and AD cohorts

	NL	% NL missing	MCI	% MCI missing	AD	% AD missing
<i>n</i>	22		56		25	
Gender, % female	36.7		35.7		32	
Age, mean (SD)	75.7 (6.1)		74.5 (7.6)		74.2 (8.6)	
ADAS-Cog 13, mean (SD)	7.5 (4.5)	4.5	17.5 (7.7)	0	27 (6.9)	16
MMSE, mean (SD)	28.8 (1.3)	0	27.3 (2)	26.8	22.8 (3.1)	20
CDR-SB, mean (SD)	0.2 (0.3)	9.1	1.9 (1.2)	26.8	5.3 (2.4)	20

NL, cognitively normal subjects; MCI, mild cognitive impairment patients; AD, Alzheimer's disease patients; ADAS-Cog 13, Alzheimer's Disease Assessment Scale-Cognitive 13 items; MMSE, Mini-Mental State Examination; CDR-SB, Clinical Dementia Rating-Sum of Boxes; *n*, number of subjects; SD, standard deviation.

for CER (Fig. 3a), PON (Fig. 3b), and SWM (Fig. 3c) reference region for PiB-positive and PiB-negative subjects (biomarker threshold derivation for PON and SWM will be discussed below). Since there were only 2 PiB+ AD subjects at Year 2, 1 PiB- AD subject at Year 1, and no PiB- AD subjects at Year 2, two-year PiB4 mean trajectory could not be fully captured for PiB+ AD cohort and could not be displayed at all for PiB- AD group. Note that the unavailability of AD subjects at 2 years was not purely drop-out related. The AD cohort was planned to be followed for 2 years initially. After we redefined our baseline according to the first PiB-PET scan available, we shifted 2 year observations to the earlier time points. Similarly, the plots in Fig. 3d–f showed mean and 95% confidence interval for changes from Baseline for CER, PON, and SWM, respectively, split by biomarker baseline status. The PiB+ group means revealed patterns as expected, with AD displaying the overall highest group mean PiB4 at any time point, NL the lowest and MCI an intermediate level for all reference regions. The variability was quite large at each time point, especially in CER-normalized settings. PiB- cohorts exhibited much lower mean levels of PiB4 over time with noticeably reduced variability compared to their respective PiB+ group. In agreement with Jack's hypothetical model of dynamic biomarkers of AD [10], 1-year rate of amyloid accumulation is higher at cognitively normal stage compared to MCI for CER and PON biomarker positive group. However, changes from baseline are much more variable for amyloid positive subjects, normalized by CER compared to PON at one and two years (Fig. 3e, f). PiB+ subgroup exhibited different trend with MCI subjects having larger one and two-year changes from baseline than NL subjects when normalized to SWM (Fig. 3d). There was a noticeable increase in amyloid accumulation over time marked with high variability in both NL and MCI PiB- subjects when normalized to CER. Biomarker negative group looked as expected at two years when normalized to PON or SWM with very small variability and almost no gain in amyloid. Thus, there may be a slight advantage to using PON or SWM as a reference region compared to CER based on the expected directionality and, most importantly, reduced variability of amyloid accumulation.

Cut-off thresholds for amyloid positivity in new reference region

In order to estimate a cut-off for biomarker positivity/negativity, we performed linear regression analysis of PON-normalized and SWM-normalized PiB4 on

CER-normalized PiB4 baseline data (Fig. 4a, b). Based on CER-based cut-off of 1.5, the cut-off values for PON and SWM were estimated to be 0.84 and 0.86, respectively.

After applying the new cut points, disagreement between PON and SWM versus CER biomarker classification was 2% and 4%, respectively. Only two MCI subjects who were classified as biomarker-positive at baseline based on CER-normalized PiB4 measure were classified as biomarker-negative by PON-normalized 4-region average (Fig. 4a). The same two MCI subjects were classified as biomarker-negative by PiB4 normalized to SWM also. There were two more MCI subjects who were classified as biomarker-negative at baseline by PiB4, normalized by CER, and classified as biomarker-positive at baseline based on the PiB4-SWM cutoff (Fig. 4b). The small classification error rates suggested that PON or SWM-normalized baseline data is consistent with CER-normalized baseline data in terms of biomarker classification. From this perspective, PON, SWM or CER were all potential candidates to serve as a reference for screening in a clinical trial.

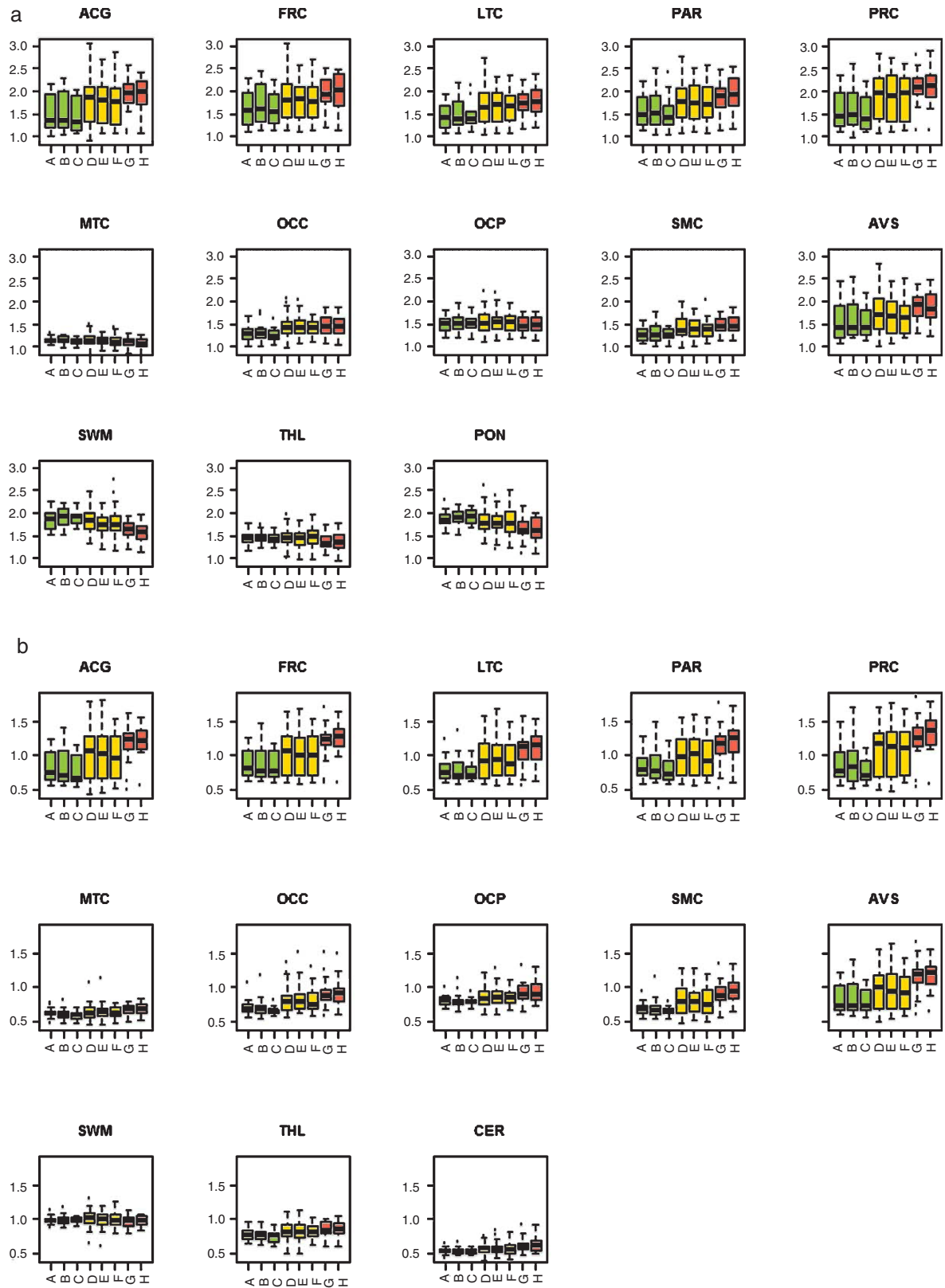
Novel composite ROIs for tracking amyloid deposition

To visualize the relationship between average amyloid accumulation and its variability we plotted the Mean/Standard Deviation (SD) against SD for 2-year change from baseline for the biomarker-positive group for each brain region for CER, PON, and SWM-normalized data (Fig. 5). In this subgroup there were 21 2-year completers for CER and SWM-normalized data and 20 for PON-normalized data. About 70% of PiB-positive subjects were MCI.

PON-normalized ROIs had the highest standardized changes from baseline and appeared to be less variable, followed by SWM, with CER-normalized ROIs having the least standardized changes from baseline and the highest standard deviation.

The specific ROIs within each group with the largest standardized change from baseline were: LTC, ACG, and FRC. PAR and PRC had moderate change from baseline and the highest variance regardless of the reference region, which made them unappealing to be included in a composite.

Based on this we calculated a novel composite measure of amyloid accumulation, PiB3, comprised of the average SUVRs of LTC, ACG and FRC, and compared it to PiB4. Based on the observed regional behavior from Fig. 5, we hypothesized that PiB3 would be a



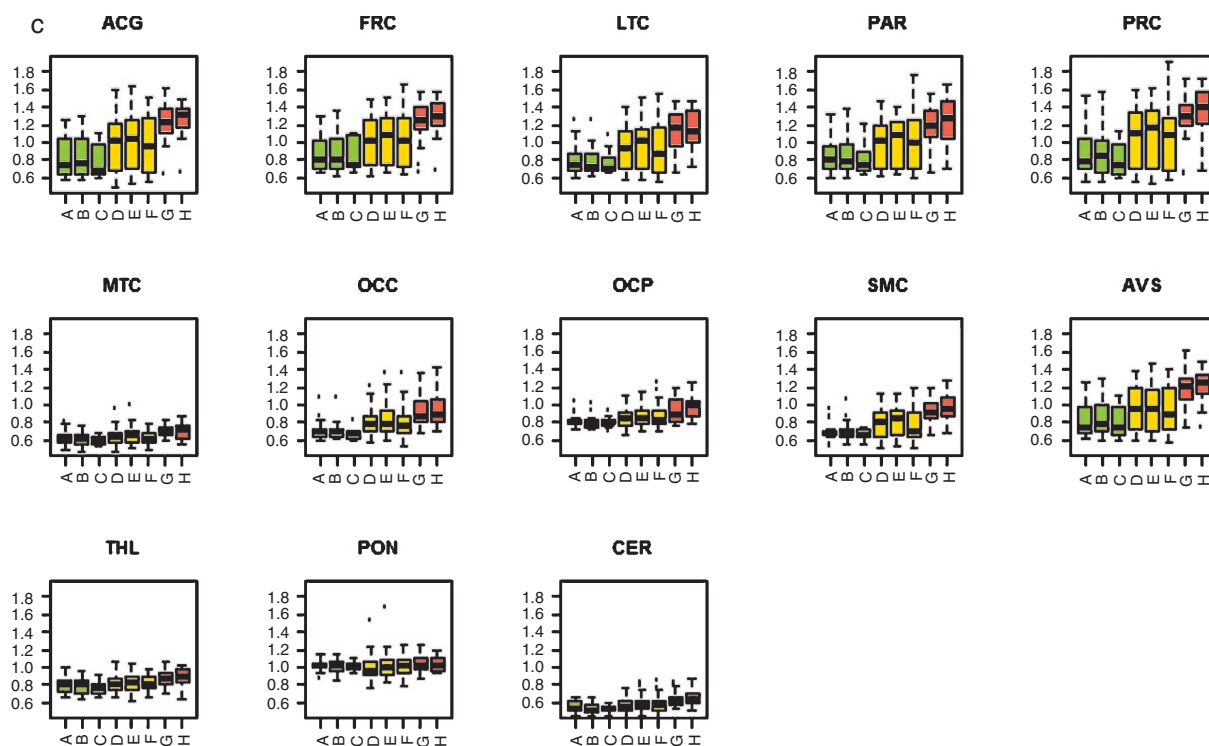


Fig. 1. (a) Boxplots of regional SUVRs, normalized to cerebellum. b) Boxplots of regional SUVRs, normalized to pons. c) Boxplots of regional SUVRs, normalized to subcortical white matter. (referenced to CER, PON, and SWM, respectively) show panels of boxplots of SUVR for each ROI (as labeled), group, and timepoint (NL (green) at baseline (A), Year 1 (B), and Year 2 (C); MCI (yellow) at baseline (D), Year 1 (E) and Year 2 (F); and AD (red), at baseline (G) and Year 1 (H)). In each plot, for each disease stage (from Cognitively Normal to AD) the 50th percentile of the boxplot traces the trend of a particular region during the observation period.

better composite measure to track amyloid deposition than PiB4 because it consisted of three regions that had the largest standardized change from baseline and appeared to be less variable compared to the rest of the regions.

Power calculations were carried out to determine how much reduction in sample sizes could potentially be achieved using improved reference regions and novel composite SUVRs. Figure 6 shows the plot of statistical power as a function of sample size for a clinical trial with 25% treatment effect for two composite measures: PiB3 and PiB4, for each of the three reference regions: CER, PON, and SWM. Mixed model was used for power calculations based on 2-year longitudinal data available for PiB+ subjects for CER, SWM, or PON-normalized data.

Novel composite PiB3 performed better than PiB4 across all three reference regions. The smallest sample sizes were noted for PON-normalized data. Assuming 25% treatment effect, the PiB3 PON-normalized SUVR would require 349 subjects per arm, 391 subjects with SWM-normalized, and 1407 with CER-

Table 3

Average sample size reduction achieved with normalizing to alternative RRs (PON and SWM, in columns) compared to CER (in rows) for conventional PiB4 and novel PiB3 composites when detecting 25% treatment effect in a two-arm parallel designed clinical trial. Sample sizes were calculated using mixed model with random slope analysis

	PiB4(PON)	PiB4(SWM)	PiB3(PON)	PiB3(SWM)
PiB4(CER)	76%	77%	85%	83%
PiB3(CER)	N/A	N/A	75%	72%

N/A, not applicable.

normalized data to achieve 80% power to detect at a $p < 0.05$ level. Table 3 indicated that the average sample size reduction with either PON or SWM RR compared to CER is about 76% for conventional PiB4 composite. By using novel PiB3 composite further improvement in sample size reduction is possible with additional 10% saving. Two-sided t -test based power analysis was also performed using 2-year completer's data, which revealed consistent with the mixed model approach sample size reduction results.

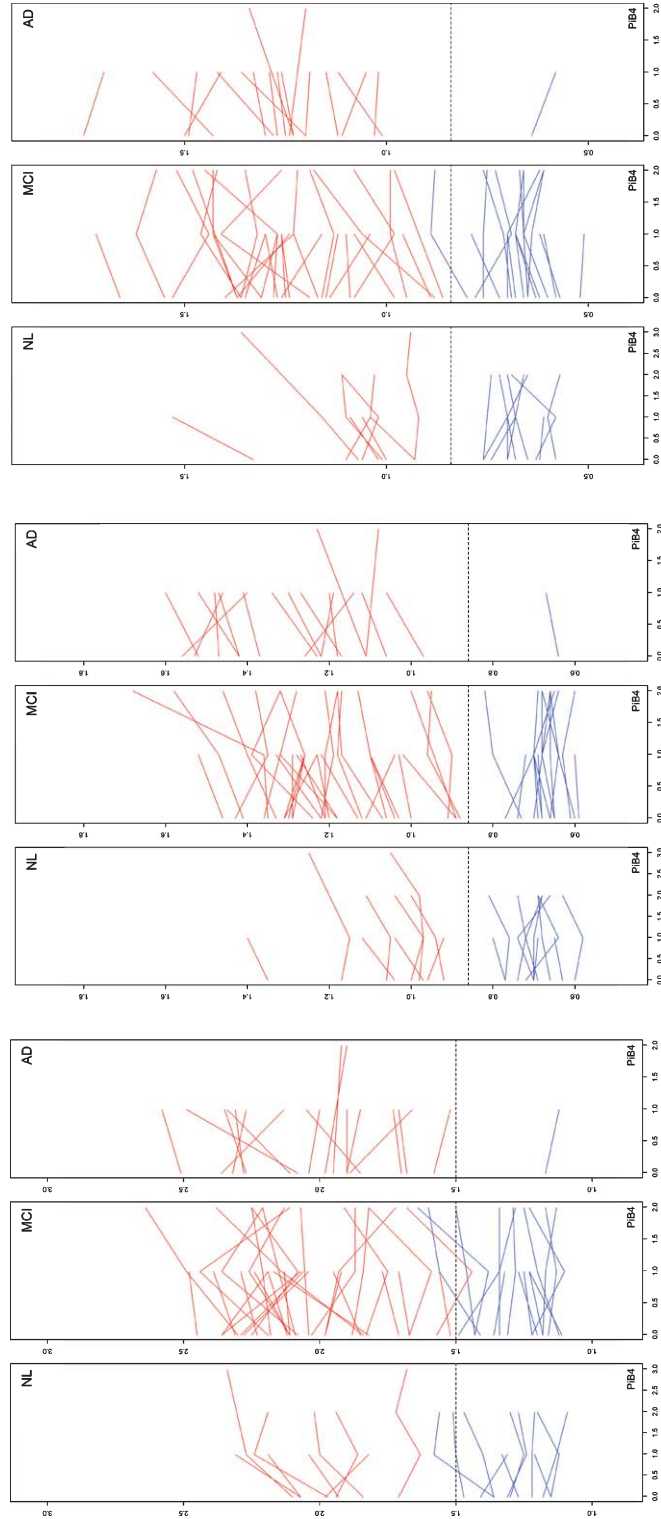


Fig. 2. PIB4 profile plots for CER (3 left panels), SWM (3 middle panels), and PON-normalized data (3 right panels). Figures below show longitudinal trajectories of amyloid accumulation across three cohorts of subjects for each of these references. For each individual we plot PIB4 on the y-axis against time in years on the x-axis, so that each line corresponds to an individual. Red/blue color codes for biomarker-positivity/negativity.

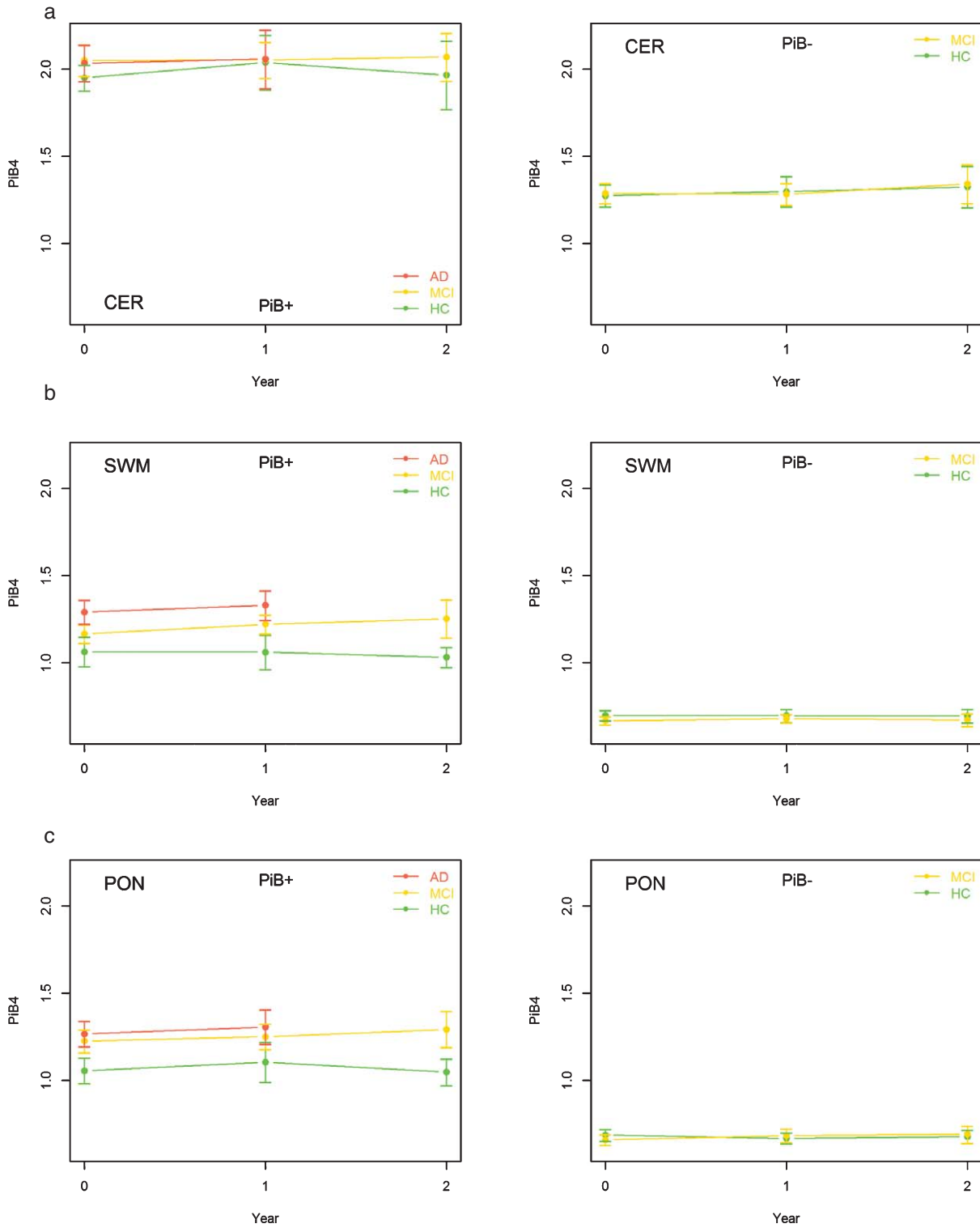


Fig. 3. (a) PiB4: Mean \pm 2*Standard Error for PiB+ (left) and PiB-(right) subgroup (top panel, CER-normalized). (b) PiB4: Mean \pm 2*Standard Error for PiB+ (left) and PiB- (right) subgroup (middle panel, SWM-normalized). (c) PiB4: Mean \pm 2*Standard Error for PiB+ (left) and PiB-(right) subgroup (bottom panel, PON-normalized).

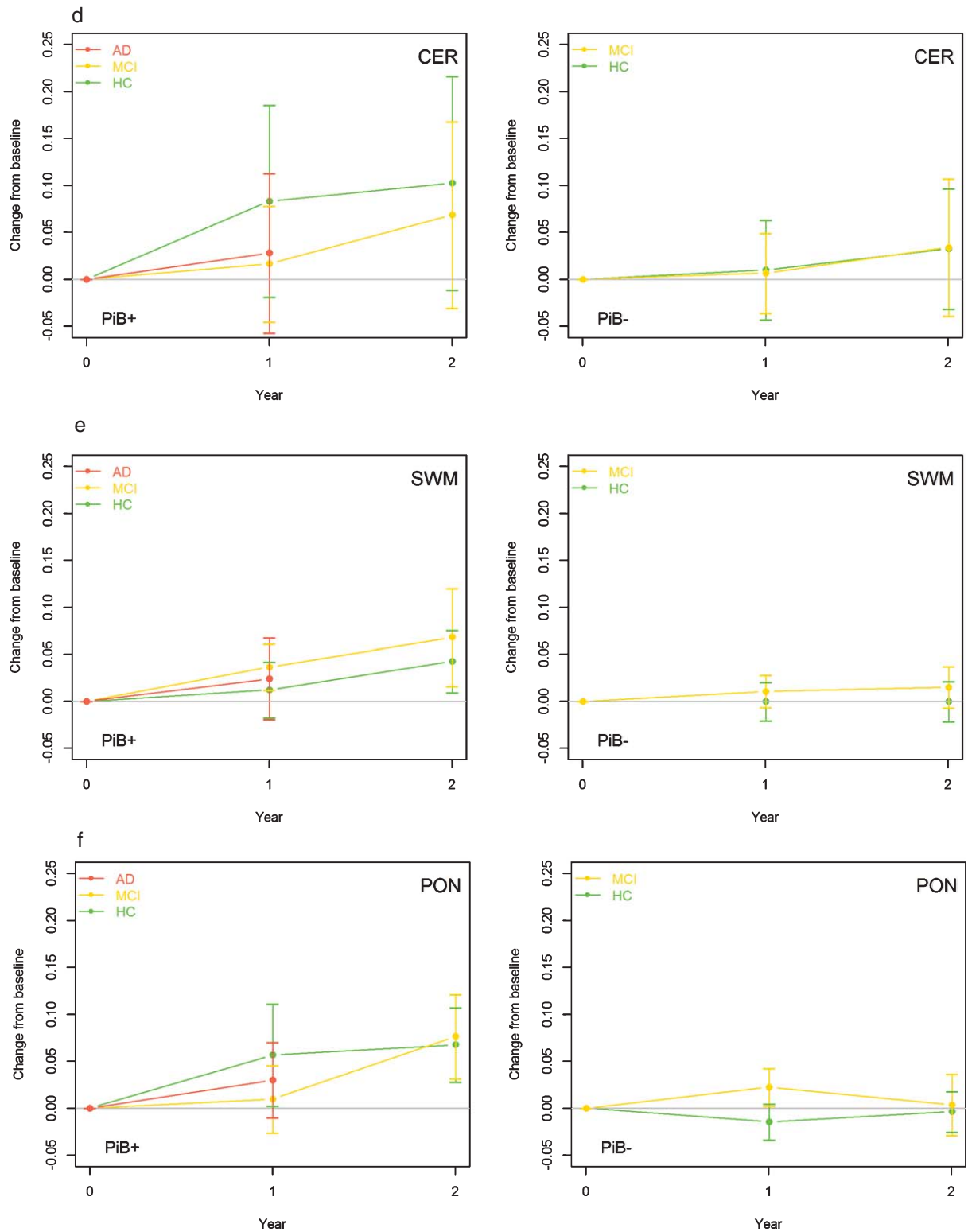


Fig. 3. (d) PiB4 change from baseline: Mean \pm 2*Standard Error for PiB+ (left) and PiB- (right) subgroup (top panel, CER-normalized). (e) PiB4 change from baseline: Mean \pm 2*Standard Error for PiB+ (left) and PiB- (right) subgroup (middle panel, SWM-normalized). (f) PiB4 change from baseline: Mean \pm 2*Standard Error for PiB+ (left) and PiB- (right) subgroup (bottom panel, PON-normalized).

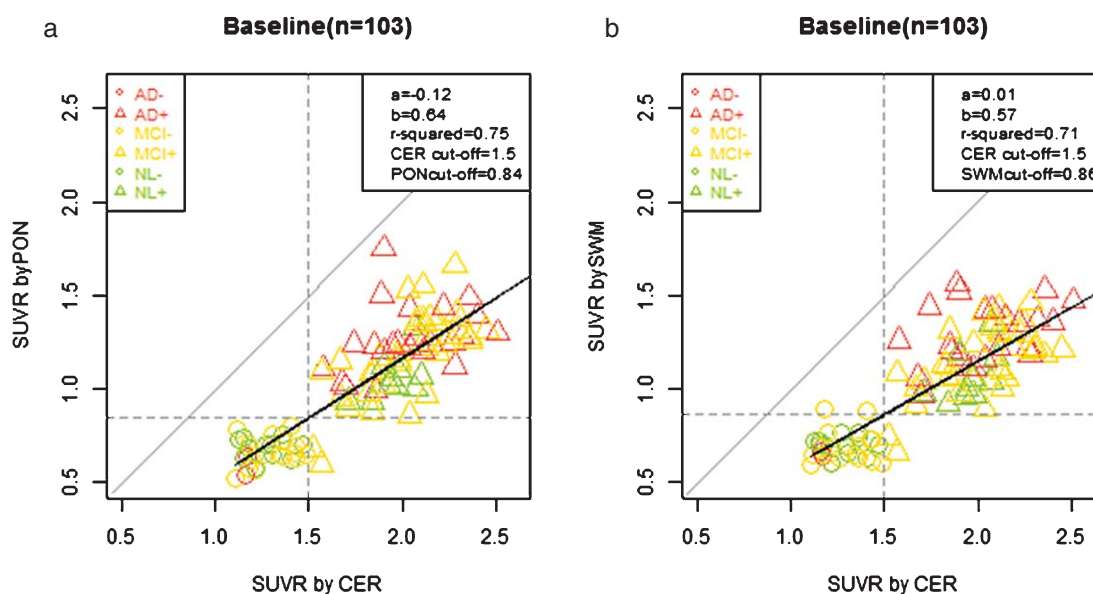


Fig. 4. (a) (left), (b) (right). Linear regression of (a) baseline PON-normalized PiB4 on baseline CER-normalized PiB4; (b) baseline SWM-normalized PiB4 on baseline CER-normalized PiB4. Symbols in a legend correspond to baseline biomarker classification, based on CER-normalized PiB4 measure, and “+” and “-” denote biomarker positivity and negativity respectively.

DISCUSSION

Working on both aspects of the SUVR composites, the denominator and the numerator, we found a potentially better reference region and SUVR composite from multiple perspectives: directionality, mean changes from baseline, while achieving consistent screening cut-offs. We evaluated the pons as an alternative reference region for normalizing amyloid-tracer signal intensity in standard ROIs, finding that the pons is consistently more stable than the cerebellum gray matter from multiple perspectives. First, individual and group mean PiB4 SUVRs display lower variability at baseline and over time for the various clinical cohorts considered (NL, MCI, and AD) when normalized to pons or subcortical white matter versus cerebellum [7, 8]. Additionally, and compellingly, the pattern of increasing amyloid accumulation with increasing disease severity for pons or subcortical white matter-normalized ROIs was consistent with expected trends of amyloid accumulation. At the same time, the lack of change in PON and SWM with disease severity suggests that they do not accumulate significant amount of amyloid. As noted earlier, the pattern of increasing amyloid accumulation with increasing disease severity was violated for cerebellum-normalized pons and subcortical white matter regions. This pattern would be manifested only in ROIs where amyloid accumulation fell below the reference ROI, leading the SUVRs for

these ROIs to decrease with time and with increasing disease severity.

Subcortical white matter and pons, which should have minimal degrees of amyloid deposition in subjects ranging from normal cognition to mild AD dementia, nonetheless had binding in excess of that seen for the cerebellum. This may result from binding of the ligand to other elements in myelinated white matter. When either of these regions was referenced to the other, binding appeared to be stable within and across disease cohorts over time, whereas binding increased in regions that are known to accumulate amyloid. The explanation for the *decreases* in SUVR in PON and SWM when normalized to cerebellum could be explained if the cerebellum is accumulating amyloid and driving down the SWM SUVRs as a result. Given the importance of a stable reference region in order to detect small changes in cortical amyloid, it is critical to identify regions with little or no amyloid accumulation to serve as reference regions. Although the SWM and the PON both appeared to be good candidates in our analyses, the development of novel tracers with increased binding to non-amyloid structure in SWM [9] may make the pons a better alternative reference region, provided that pons is relatively spared from non-specific uptake.

Conventional cut-offs to demarcate amyloid-positive from amyloid-negative have been developed using cerebellum normalization. We proposed to

itudinal cohort would be desirable to confirm the findings.

ACKNOWLEDGMENTS

Data collection and sharing for this project was funded by the Alzheimer's Disease Neuroimaging Initiative (ADNI) (National Institutes of Health Grant U01 AG024904) and DOD ADNI (Department of Defense award number W81XWH-12-2-0012). ADNI is funded by the National Institute on Aging, the National Institute of Biomedical Imaging and Bioengineering, and through generous contributions from the following: Alzheimer's Association; Alzheimer's Drug Discovery Foundation; BioClinica, Inc.; Biogen Idec Inc.; Bristol-Myers Squibb Company; Eisai Inc.; Elan Pharmaceuticals, Inc.; Eli Lilly and Company; F. Hoffmann-La Roche Ltd and its affiliated company Genentech, Inc.; GE Healthcare; Innogenetics, N.V.; IXICO Ltd.; Janssen Alzheimer Immunotherapy Research & Development, LLC.; Johnson & Johnson Pharmaceutical Research & Development LLC.; Medpace, Inc.; Merck & Co., Inc.; Meso Scale Diagnostics, LLC.; NeuroRx Research; Novartis Pharmaceuticals Corporation; Pfizer Inc.; Piramal Imaging; Servier; Synarc Inc.; and Takeda Pharmaceutical Company. The Canadian Institutes of Health Research is providing funds to support ADNI clinical sites in Canada. Private sector contributions are facilitated by the Foundation for the National Institutes of Health (<http://www.fnih.org>). The grantee organization is the Northern California Institute for Research and Education, and the study is coordinated by the Alzheimer's Disease Cooperative Study at the University of California, San Diego. ADNI data are disseminated by the Laboratory for Neuro Imaging at the University of Southern California.

We would like to thank March Schmidt for his support and encouragement of this work.

Authors' disclosures available online (<http://www.j-alz.com/disclosures/view.php?id=2421>).

REFERENCES

- [1] Klunk WE, Engler H, Norberg A, Wang Y, Blomqvist G, Holt DP, Bergstrom M, Savitcheva I, Huang GF, Estrada S, Ausen B, Debnath ML, Barletta J, Price JC, Sandell J, Lopresti BJ, Wall A, Koivisto P, Antoni G, Mathis CA, Langstrom B (2004) Imaging brain amyloid in Alzheimer's disease with Pittsburgh compound-B. *Ann Neurol* **55**, 306-319.
- [2] Klunk WE, Wang Y, Huang GF, Debnath ML, Holt DP, Mathis CA (2001) Uncharged thioflavin-T derivatives bind to amyloid-beta proteins with high affinity and readily enter the brain. *Life Sci* **69**, 1471-1484.
- [3] Price JC, Klunk WE, Lopresti BJ, Lu X, Hoge JA, Ziolkowski SK, Holt DP, Meltzer CC, DeKosky ST, Mathis CA (2005) Kinetic modeling of amyloid binding in humans using PET imaging and Pittsburgh compound-B. *J Cereb Blood Flow Metab* **25**, 1528-1547.
- [4] Verhoeff NP, Wilson AA, Takeshita S, Trop L, Hussey D, Singh K, Kung HF, Kung MP, Houle S (2004) *In-vivo* imaging of Alzheimer disease beta-amyloid with [¹¹C]SB-13 PET. *Am J Geriatr Psychiatry* **12**, 584-595.
- [5] Jagust WJ, Bandy D, Chen K, Foster NL, Landau SM, Mathis CA, Price JC, Reiman EM, Skovronsky D, Koeppe RA, Alzheimer's Disease Neuroimaging Initiative (2010) The Alzheimer's Disease Neuroimaging Initiative positron emission tomography core. *Alzheimers Dement* **6**, 221-229.
- [6] Aizenstein HJ, Nebes RD, Saxton JA, Price JC, Mathis CA, Tsopelas ND, Ziolkowski SK, James JA, Snitz BE, Houck PR, Bi W, Cohen AD, Lopresti BJ, DeKosky ST, Halligan EM, Klunk WE (2008) Frequent amyloid deposition without significant cognitive impairment among the elderly. *Arch Neurol* **65**, 1509-1517.
- [7] Lundqvist R, Lilja J, Thomas BA, Lotjonen J, Villemagne VL, Rowe CC, Thurfjell L (2013) Implementation and validation of an adaptive template registration method for F-Flutemetamol imaging data. *J Nucl Med* **54**, 1472-1478.
- [8] Edison P, Hinz R, Ramlackhansingh A, Thomas J, Gelosa G, Archer HA, Turkheimer FE, Brooks DJ (2012) Can target-to-pons ratio be used as a reliable method for the analysis of [¹¹C] PIB brain scans? *Neuroimage* **60**, 1716-1723.
- [9] Clark CM, Schneider JA, Bedell BJ, Beach TG, Bilker WB, Mintun MA, Pontecorvo MJ, Hefti F, Carpenter AP, Flitter ML, Krautkramer MJ, Kung HF, Coleman RE, Doraiswamy PM, Fleisher AS, Sabbagh MN, Sadowsky CH, Reiman PE, Zehntner SP, Skovronsky DM, AV45-A07 Study, Group (2011) Use of florbetapir-PET for imaging beta-amyloid pathology. *JAMA* **305**, 275-283.
- [10] Jack CR Jr, Knopman DS, Jagust WJ, Shaw LM, Aisen PS, Weiner MW, Petersen RC, Trojanowski JQ (2010) Hypothetical model of dynamic biomarkers of the Alzheimer's pathological cascade. *Lancet Neurol* **9**, 119-128.
- [11] Villemagne VL, Burnham S, Bourgeat P, Brown B, Ellis KA, Salvado O, Szoek C, Macaulay SL, Martins R, Maruff P, Ames D, Rowe CC, Masters CL, Australian Imaging Biomarkers and Lifestyle (AIBL) Research Group (2013) Amyloid beta deposition, neurodegeneration, and cognitive decline in sporadic Alzheimer's disease: A prospective cohort study. *Lancet Neurol* **12**, 357-367.
- [12] Raghavan N, Samtani MN, Farnum M, Yang E, Novak G, Grundman M, Narayan V, Diernardo A, the Alzheimer's Disease Neuroimaging Initiative (2013) The ADAS-Cog revisited: Novel composite scales based on ADAS-Cog to improve efficiency in MCI and early AD trials. *Alzheimers Dement* **9**(1 Suppl), S21-S31.